NEOPLASIA
www.neoplasia.com
Volume 22 Number 11 October 2020 pp. 539–553

The anti-B7-H4 checkpoint synergizes trastuzumab treatment to promote phagocytosis and eradicate breast cancer

Xiaochen Hu [a,b]; Yiwen Liu [b]; Xiusen Zhang [b]; Dejiu Kong [a,b]; Jinyu Kong [b]; Di Zhao [a,b]; Yibo Guo [b]; Lingyun Sun [b]; Luoyi Chu [b]; Shupei Liu [b]; Xurong Hou [a,b]; Feng Ren [c]; Ying Zhao [c]; Chengbiao Lu [c]; Desheng Zhai [c]; Xiang Yuan [a,b,*]

[a] Department of Medical Oncology, Cancer Hospital, The First Affiliated Hospital, College of Clinical Medicine, Medical College of Henan University of Science and Technology, Luoyang 471003, China; [b] Henan Key Laboratory of Cancer Epigenetics, Cancer Hospital, The First Affiliated Hospital, College of Clinical Medicine, Medical College of Henan University of Science and Technology, Luoyang 471003, China; [c] Department of Pathology, Xinxiang Medical University, Xinxiang 453003, China

Abstract

Trastuzumab is a humanized mAb used to treat *HER2*-overexpressing breast cancer; however its mechanisms remain to be fully elucidated. Previous studies suggest a role for immunity in mediating trastuzumab-specific antitumor effects. This study evaluated the role(s) of trastuzumab and other antibodies on macrophage activation and Ab-dependent cell-mediated phagocytosis (ADCP) of HER2$^+$ breast cancer cells *in vitro* and *in vivo*. We employed orthotopic implantation of HER2$^+$ murine breast cancer (BC) cells in immunocompetent mouse models, a human HER2$^+$ BC xenograft in an immune humanized mouse model, and human PDXs involving adoptive transfer of autologous macrophages to simulate an endogenous mammary tumor-immune microenvironment. Our study demonstrated that trastuzumab greatly and consistently increased macrophage frequency and tumor-cell phagocytosis, and that concurrent knockdown of B7-H4 by a neutralizing antibody increased immune cell infiltration and promoted an antitumor phenotype. Furthermore, neoadjuvant trastuzumab therapy significantly upregulated B7-H4 in the cancer-infiltrating macrophages of HER2$^+$ BC patients, which predicted poor trastuzumab response. We suggest that strategies to specifically enhance ADCP activity might be critical to overcoming resistance to HER2 mAb therapies by inhibiting tumor growth and potentially enhance antigen presentation. Furthermore, these results advance the understanding of macrophage plasticity by uncovering a dual role for ADCP in macrophages involving elimination of tumors by engulfing cancer cells while causing a concomitant undesired effect by upregulating immunosuppressive checkpoints.

Neoplasia (2020) 22 539–553

Keywords: HER2$^+$ breast cancer, Trastuzumab, Macrophages, ADCP, B7-H4

Introduction

Trastuzumab is a humanized monoclonal antibody (mAb) used to treat *HER2*-overexpressing breast cancer [1]. Despite years of successful clinical use, the mechanisms of trastuzumab action are still being investigated [2]. Although suppression of HER2 signaling was a primary focus of early mechanistic studies [3], subsequent studies have focused on the role of immunity in mediating trastuzumab-specific antitumor effects [4]. However, the clinical benefit associated with HER2 mAb therapies in patients with HER2$^+$ BC remains heterogeneous and critical. Consequently, understanding the associated antitumor mechanisms could enable rational strategies to enhance its efficacy and overcome resistance.

The established modes of trastuzumab action include the inhibition of HER2-mediated cell signalling [5] and antibody (Ab)-dependent cell-mediated cytotoxicity (ADCC) [6] and phagocytosis (ADCP) [7]. ADCC has been studied extensively and is critical for the tumoricidal effects of therapeutic antibodies that allow immune cells bind to cancer cells and lyse them by releasing perforin and granzymes [8]. In particular, studies show that interaction between anti-HER2 antibodies and Fcγ receptors (FCGRs) expressed on immune cells, such as neutrophils [9], T cells [10], and natural killer (NK) cells [11,12], might be involved in the

* Corresponding author at: Henan Key Laboratory of Cancer Epigenetics, Cancer Institute, The First Affiliated Hospital, College of Clinical Medicine of Henan University of Science and Technology, 24 Jinghua Road, Jianxi District, Luoyang, Henan 471003, China.
e-mail address: yuanxiangdrive@163.com (X. Yuan).

© 2020 The Authors. Published by Elsevier Inc. on behalf of Neoplasia Press, Inc. This is an open access article under the CC BY-NC-ND license (http://creativecommons.org/licenses/by-nc-nd/4.0/).
https://doi.org/10.1016/j.neo.2020.08.007

therapeutic activity of trastuzumab. Consistent with this observation, macrophages are essential for Ab-dependent depletion of cancer cells [13]. However, the mechanisms of macrophage response to trastuzumab and associated antitumor efficacy have not been fully established. Therefore, this study clarified the role of macrophages and ADCP in trastuzumab-mediated antitumor activity.

B7-H4 (B7x, B7S1) is a recently discovered member of the B7 family of T cell costimulatory molecules [14]. Our recent study demonstrated that blockade of B7-H4 in cancer cells confers protective $CD8^+$ T cell immunity against infection with pathogens [15]. Because B7-H4 was previously described as a critical immune-checkpoint molecule in macrophages that determines host responses [16], we investigated the possibility that B7-$H4^+$ tumor macrophages constitute a novel suppressor cell population in BC and determined a role for B7-H4 in limiting the ADCP effect of trastuzumab against $HER2^+$ human BC. Our findings support the importance of ADCP in enabling trastuzumab-mediated treatment of BCs and suggest the therapeutic potential of utilizing B7-H4 checkpoint blockade in combination with trastuzumab for achieving durable $HER2^+$ BC control.

Materials and methods

Study participants

This study was performed at the First Affiliated Hospital of Henan University of Science and Technology (HUST; Luoyang, Henan, China). Patients were enrolled from 2006 to 2012 with complete follow-up data and histopathologic slides. Prior to sample collection, informed consent was obtained from all patients in accordance with the protocols approved by the institutional review boards of HUST. All procedures involving patients were performed in accordance with the Declaration of Helsinki [17]. We enrolled 116 BC patients undergoing surgery, with all cases confirmed by pathologic diagnosis and determined as $HER2^+$ BC (stage I–III) according to 3+ staining by immunohistochemical (IHC) analysis (Herceptest; Dako, Glostrup, Denmark) or HER2 amplification by fluorescence in situ hybridization (Pathvysion HER2 test; Abbott/Vysis, Des Plaines, IL, USA) by the Pathology Department of HUST. All patients received neoadjuvant therapy. Among them, 58 patients received trastuzumab-containing neoadjuvant treatment, and the other 58 received neoadjuvant chemotherapy without trastuzumab. The neoadjuvant treatment regimens were as follows: doxorubicin 60 mg/m^2 plus cyclophosphamide 600 mg/m^2 every 3 weeks for four cycles, followed by paclitaxel (80 mg/m^2) with or without trastuzumab (initial loading dose of 4 mg/kg/week and subsequent doses of 2 mg/kg/w) administered weekly for 12 weeks; or docetaxel 75 mg/m^2 and cyclophosphamide 600 mg/m^2 with or without trastuzumab (initial loading dose of 8 mg/kg and subsequent doses of 6 mg/kg) every 3 weeks for four to six cycles. There was no significant difference in chemotherapy constitution or basic conditions between the groups with or without trastuzumab. Therapeutic effects were evaluated according to the standard of RECIST (Response Evaluation Criteria in Solid Tumors). Complete response (CR) was defined as disappearance of all lesions in both primary tumor and lymph nodes, partial response (PR) was defined as at least a 30% reduction in the sum of the longest diameter of target lesions, progressive disease (PD) was defined as at least a 20% increase in the sum of the longest diameter of target lesions; and stable disease was defined as neither sufficient shrinkage to qualify as PR nor sufficient increase to qualify as PD. CR and PR were classified as treatment sensitive, whereas stable disease and PD were classified as treatment resistant. Paired biopsy samples and surgical resected samples were collected from the same patient before and after neoadjuvant treatments. Each specimen was sufficient to be cut into pieces and treated differently for various uses, transferred to liquid nitrogen for RNA extraction for sequencing, or fixed in 10% formaldehyde for paraffin embedding. Additional fresh BC specimens were collected for generation of patient-derived xenografts (PDXs). Monocytes were isolated and sorted from heparinized venous blood samples after trastuzumab neoadjuvant therapy for co-culture and adoptive-transfer studies, as well as development of the humanized mouse model.

Cell culture conditions

The $HER2^+$ BC cell lines MM3MG-HER2Δ16, SKBR3, and BT-474 were maintained in our laboratory. Cell lines were cryopreserved in aliquots or maintained at a density of 5×10^5 cells/mL in RPMI-1640 medium (GE Healthcare, Pittsburgh, PA, USA) supplemented with 10% fetal bovine serum (FBS; GE Healthcare) in an incubator at 37 °C and 5% CO_2. To help prevent or control contamination with mycoplasma, an anti-mycoplasma reagent (InvivoGen, San Diego, CA, USA) was used prophylactically at a working concentration of 2.5 μg/mL [18]. All cells were maintained or passaged for <3 months prior to cryopreserving aliquots for further procedures. Short tandem repeat profiling was performed by GENEWIZ (Suzhou, China) to authenticate the cell lines. Peripheral blood monocytes were isolated by Ficoll density gradient centrifugation. Macrophages were obtained by culturing monocytes in DMEM medium (GIBCO, Gaithersburg, MD, USA) supplemented with 10 ng/mL M-CSF (Cat# 11792-HNAH; Sino Biological Inc., Beijing, China) and 10% FBS (GIBCO) for 6 days. In some experiments, macrophages were treated with 10 ng/mL interleukin (IL)-1β, IL-18, GM-CSF, IL-8, IL-6, CCL2, CCL8, CCL17, CCL18, or CXCL1 (PeproTech, Cranbury, NJ, USA). $CD8^+$ T cells, naive $CD4^+$ T cells, and NK cells were isolated by magnetic activated cell sorting using direct CD8 and CD56 isolation kits (Cat# 130-094-156 and 130-050-401; Miltenyi Biotec, Bergisch Gladbach, Germany) and a naive $CD4^+$ T cell isolation kit II (Cat# 130-094-131; Miltenyi Biotec) according to manufacturer instructions. Neutrophils were isolated by positive selection of $CD66b^+$ cells with microbeads (Cat# 130-104-913; Miltenyi Biotec). $CD8^+$ T cells, $CD4^+$ T cells, and NK cells were cultured in RPMI-1640 medium (GIBCO) supplemented with 25 mM HEPES, 4 mM L-glutamine, 25 μM 2-mercaptoethanol, and 10% FBS at 37 °C, with the media replaced every 2 days. The purity of cell populations was confirmed at >90% by flow cytometry. Additionally, we obtained tumor-specific $CD8^+$ and $CD4^+$ T cells. Briefly, monocytes were cultured in DMEM supplemented with 25 ng/mL GM-CSF (Cat# 300-03-20; PeproTech), 5 ng/mL IL-4 (Cat# 200-04-20; PeproTech), and 10% FBS for 5 days.

Mice

NOD/SCID IL2γ$c^{-/-}$ (NSG) and BALB/c mice (Biocytogen, Beijing, China) were housed under specific pathogen-free conditions at the Animal Care Facility of Henan University of Science and Technology. All procedures involving animals were approved and monitored by the Animal Care and Use Committee of the Henan University of Science and Technology.

Generation of genetically modified cells

For B7-H4 knockdown (KD) in macrophages, the RNAi Consortium lentiviral B7-H4 short-hairpin RNA (shRNA) was acquired from Thermo Fisher Scientific (Fremont, CA, USA). To package the lentivirus, HEK 293T cells were co-transfected with B7-H4 shRNA plasmid psPAX2 and the PMD2.G envelope plasmid using 293fectin transfection reagent (Invitrogen, Carlsbad, CA, USA), as previously described[19]. At 48 h, the virus was collected to infect the macrophages in the presence of polybrene (4 μg/mL; Sigma-Aldrich, St. Louis, MO, USA). Three days after infection, the cells were selected by puromycin (Sigma-Aldrich), the

selected cells were amplified, and B7-H4 KD was confirmed by flow cytometry. Macrophages were transfected with wild-type (WT) B7-H4 (Upstate), and B7-H4-expressing clones were selected using neomycin. To evaluate the effect of B7-H4 expression on tumor growth and HER2 mAb therapy *in vivo*. We implanted PDXs from surgical HER2$^+$ BC specimens with or without trastuzumab neoadjuvant therapy into NSG mice engrafted with macrophages from the corresponding patient. Macrophages expressing considerably higher levels of B7-H4 after trastuzumab-containing neoadjuvant therapy were collected and used for B7-H4 knockdown; whereas, macrophages from pre-treatment BC biopsies expressing undetectable B7-H4 were used for B7-H4 overexpression and adoptive transfer. To create a transformed BALB/c mammary cell line dependent on human HER2 signaling, cell derived from the mouse mammary cell line MM3MG expressing a highly oncogenic isoform of human HER2 (HER2Δ16) were generated by retroviral transduction, followed by positive selection using puromycin and limiting dilution

Flow cytometry analysis

Cells were stained with the following fluorochrome-conjugated mAbs: human B7-H4 (eBioscience, San Diego, CA, USA), human CD8, human CD56 (Cat# 318310; BioLegend, San Diego, CA, USA), human CD14 (Cat# 301804; BioLegend), F4/80 (BM8; BioLegend), CD11b (m1/70; BD Biosciences, San Jose, CA, USA), human perforin (Cat# 308106; BioLegend), human granzyme B (Cat# 515403; BioLegend), human CD45 (Cat# 304011; BioLegend), and mouse CD45 (Cat# 103107; BioLegend). Intracellular cytokine staining was performed using an intracellular fixation and permeabilization kit (Cat# 88-8824; eBioscience) according to manufacturer instructions. Macrophages were identified as F4/80$^+$/CD11b$^+$, and Ly-6G lymphocytes were analyzed by first excluding F4/80$^+$/CD45$^+$ macrophages and dead cells (7AAD$^+$), followed by CD45 selection, with T cells either CD4$^+$ or CD8a$^+$. For some experiments, we used an apoptosis detection kit (Cat# 640932; BioLegend), as previously described [20]. The samples were analyzed using a Beckman CytoFLEXFlow cytometer (Beckman Coulter, Brea, CA, USA), and data were analyzed by FlowJo software (Becton Dickinson, Franklin Lakes, NJ, USA).

Histologic analyses of BC

For histopathology, stored BC tissues fixed in 4% neutral-buffered formaldehyde were embedded in paraffin, cut into longitudinal sections (4 μm), and stained with hematoxylin-eosin. Examination of the tissue sections for histopathological lesions, including the occurrence of infiltrates of polymorphonuclear and mononuclear cells, erosive lesions, and edema, was performed blind. Staining intensity was classified using the following numerical scale: grade 0 (none, 0–10% staining); grade 1 (weak, 10–30%); grade 2 (moderate, 30–60%), and grade 3 (strong, >60% staining). A score $\geq$2 was considered positive staining, previously described [21]. The number of immunostained cells in four fields per specimen was counted using a light microscope (Eclipse 80i; Nikon, Tokyo, Japan) at 400× magnification. Quantitative descriptions of each score were defined as follows: 1, 100 þ 20 cells/mm^2; 2, 200 þ 40 cells/mm^2; 3, 400 þ 80 cells/mm^2; and 4, 800 þ 160 cells/mm^2. Specimens were incubated with anti-B7-H4 (Cat# ab209242; Abcam, Cambridge, UK); human CD4 (Cat# ab133616; Abcam), mouse CD4 (Cat# ab183685), human CD8 (Cat# ab4055; Abcam), mouse CD8 (Cat# ab22378; Abcam), mouse anti-human CD68 (1:100; Cat# ab955; Abcam), mouse anti-human CD56 (1:100; Cat# MA1-06801; Thermo Fisher Scientific), rabbit anti-human HER2 (Cat# 2165; Cell Signaling Technology, Danvers, MA, USA), or rat anti-mouse CD49b (1:50; Cat# 108901; BioLegend) at 4 °C overnight. This was followed by washing with PBS and staining with a rabbit anti-mouse IHC secondary antibody kit (Cat# GK500705; Gene Tech, Shanghai, China) or anti-rat IHC secondary antibody kit (Cat# 7077; Cell Signaling Technology) according to manufacturer instructions.

Development of a humanized mouse model of BC

Monocytes were purified from the peripheral blood of cancer patients from whom PDXs had been generated and isolated by Ficoll density gradient centrifugation. Macrophages were obtained by culturing monocytes in DMEM medium (GIBCO) supplemented with 10 ng/mL M-CSF (Cat# 11792-HNAH; Sino Biological Inc.) and 10% FBS (GIBCO) for 6 days. In some experiments, macrophages were treated with 10 ng/mL IL-1β, IL-18, GM-CSF, IL-8, IL-6, CCL2, CCL8, CCL17, CCL18, or CXCL1 (PeproTech). Briefly, monocytes were cultured in DMEM supplemented with 25 ng/mL GM-CSF (Cat# 300-03-20; PeproTech), 5 ng/mL IL-4 (Cat# 200-04-20; PeproTech), and 10% FBS for 5 days. NSG mice were then sublethally irradiated with 200 cGy. We isolated patient peripheral blood CD34$^+$ hematopoietic stem cells (HSCs) [22] using Ficoll-Paque Plus (GE Healthcare) hypaque centrifugation and a positive selection kit (Cat# 17856; Stemcell Technologies, Vancouver, Canada). The HSCs were then expanded in stem cell serum-free medium (Cat. No. 09655; Stemcell Technologies) and transplanted (200 μL of 4×10^6 cells/mL) into 40 irradiated 2- to 4-month-old female mice via tail vein injection. At 30-days after bone marrow transplantation, the proportions of peripheral human versus mouse CD45$^+$ cells were monitored by fluorescence-activated cell sorting (FACS) to assess reconstitution, as previously described [15]. We calculated chimerism as follows: % CD45$^+$ human cells/total cells (human CD45$^+$ cells plus mouse CD45$^+$ cells). At 45 days after HSC transplantation, we implanted a 1 mm × 2 mm fragment of a PDX obtained from a BC patient and previously grown in the fourth mammary fat pad of each of the 40 NSG mice (20 mice per patient tumor) that had been engrafted with CD34$^+$ HSCs from that patient. When the diameter of the PDX reached 5 mm × 5 mm in mice with human CD45$^+$ cells constituting >30% of peripheral blood cells, the mice were dosed according to the schedule outlined in the following section. The tumor-bearing mice received intravenous infusions of expanded peripheral monocytes from the patient (100 μL of 2×10^6 cells/mL) for an additional 2 weeks, after which we euthanized the mice, removed the tumors for volume determination, and allocated them for histology and FACS analysis of infiltrating monocytes and leukocytes.

In vivo tumor studies

Fragments of BC PDXs (1–2 mm) were implanted subcutaneously into the flank region of humanized mice, and individual animals with palpable breast tumors (~200 mm^3) were enrolled in a specific treatment group (n = 10/group). Mouse anti-human HER2 Ab (4D5), mouse immunoglobulin G (IgG)1 [kindly provided by Genetech (San Francisco, CA, USA)], and trastuzumab (Roche, Basel, Switzerland) or human IgG1 (Cat# 0151K-01; SouthernBiotech, Birmingham, AL, USA) was intravenously injected at a loading dose of 4 μg/g, followed by weekly injections of 2 μg/g into HER2$^+$ mice and humanized mice, respectively, mimicking human dosing regimens. For anti-B7-H4 combination therapy, 100 μg anti-B7-H4 (188; Cat# No. 16-5972-81; eBioscience) (100 μg/mouse by weekly intraperitoneal injection) was injected intraperitoneally on the day of anti-neu treatment. The animals dosed according to the appropriate schema (n = 10 mice/group) were monitored daily for up to 2 months, and the objective response and survival rates were recorded. An additional cohort of mice (n = 5/group) was included to conduct mechanistic studies. In this cohort, the mice were sacrificed on day 30 post-tumor inoculation. Residual tumors were surgically removed before terminal escape (tumor with PR) or CR and processed for IHC and flow

cytometric analysis. Results related to immune infiltration were determined, and a representative mouse from each treatment group in this separate cohort was measured for tumor volume (TV): TV (mm^3) = $\pi/6 \times$ length $\times$ width^2. Mice suffering from progressive disease or those used for subsequent analysis were euthanized when the TV was >2,500 mm^3. CR was defined as complete regression of the tumor without any recurrence.

Generation of tumor-infiltrating lymphocytes

BC PDXs were minced into small pieces and digested with a triple-enzyme mixture containing collagenase type IV (0.5 mg/mL; Sigma-Aldrich), hyaronidase (0.5 mg/mL; Sigma-Aldrich), and deoxyribonuclease (0.02 mg/mL; Sigma-Aldrich) for 120 min at room temperature. After digestion, BC cells were washed twice in PBS and cultured in RPMI-1640 containing 10% human serum supplemented with L-glutamine (Sigma-Aldrich), 2-mercaptethanol (Sigma-Aldrich), and IL-2 (1000 U/mL; Cat# 130-097-742; Miltenyi Biotec) for T cell generation. Following release of T cells from tumor tissues, they were grown in high-dose IL-2 (1000 U/mL)-containing medium for 1 week, followed by transfer to a fresh well and growth in low-dose IL-2 (50 U/mL)-containing medium.

Generation of tumor-infiltrating mononuclear cells

Briefly, tumor xenografts were minced into small (1–2 mm) pieces and digested with 0.125% trypsin for 30–40 min at 37 °C under constant shaking. The cells were sequentially filtered through 500-μm, 100-μm, and 70-μm mesh cell strainers and centrifuged at 2500 rpm for 15 min using a 1-mL cell suspension above 5 mL of 45% Percoll in the middle and 5 mL of 60% Percoll at the bottom in a 15-mL tube. Mononuclear cells were collected from the cell layer in the interphase between 45% and 60% Percoll, and isolated cells were analyzed for human reconstitution by flow cytometry. We used an ``adoptive monocyte transfer'' model, in which tumors from BC patients who had received neoadjuvant trastuzumab-based therapy were orthotopically implanted into the mammary fat pad of NSG mice previously engrafted with monocytes from the same patient. Mouse therapies (as indicated in the phased regimen) were initiated prior to monocyte transfusion. Mice were euthanized at the indicated days post-transfer, tissues were harvested and digested into single-cell suspensions and flow cytometry was performed to examine the proportion of tumor-infiltrating macrophages ($F4/80^+Gr1^-CD11b^+$).

Generation of bone marrow-derived macrophages (BMMs) and stimulation of different types of macrophages in vitro

BMMs were differentiated from bone marrow cells. Briefly, isolated bone marrow cells were cultured in complete RPMI-1640 medium supplemented with 10% fetal calf serum and 30% pre-tested conditioned medium (CM) from the L929 cell line as a source of M-CSF for 5 days. BMMs were confirmed as >95% $CD11b^+$ according to flow cytometry. The BMMs were further polarized to type 1 macrophages (M1) by addition of interferon (IFN)-γ (50 ng/mL) and lipopolysaccharide (10 ng/mL) and to type 2 macrophages (M2) by addition of IL-4 (20 ng/mL) [23–27]. CM from BC cell culture (3 days) was used to polarize BMMs to macrophages derived with cancer cell CM (Mcm).

ADCP assay using flow cytometry

For two-color flow cytometry assays of *in vivo* phagocytosis, $HER2^+$ murine MM3MG-HER2Δ16 cells were labeled with a lipophilic membrane dye (DiO/DiD, 5 μM; Invitrogen) for 30 min at 37 °C. When the tumors were palpable, the animals were treated with the indicated therapy. At the end of treatment, cells were stained with FITC-anti-CD11b (BD Biosciences) for 30 min at 4 °C and analyzed by flow cytometry. Cells were gated for $CD11b^+$ cells (macrophages), which were then grouped as single-positive macrophages alone (DiD^-, $CD11b^+$) and two-color stained phagocytosed macrophages (DiD^+, $CD11b^+$). The percentage of phagocytosis was calculated as the population of phagocytized macrophages among total macrophages. All tests were performed in triplicate, and the results were expressed as the mean þ SD. For the two-color flow cytometry assays of *in vitro* phagocytosis, $HER2^+$ BC cells (1×10^5) pre-dyed with CellTracker Deep Red (CTDR) dye (Cat# C34565; Thermo Fisher Scientific) were co-cultured with macrophages pre-dyed with CellTracker 5-chloromethylfluorescein diacetate (CMFDA) dye (Cat# C7025; Thermo Fisher Scientific) with or without trastuzumab (Roche), respectively. The ratios of BC cells to macrophages were 1:5 (without trastuzumab) and 3:1 (with trastuzumab). After 24 h, the cells were rigorously washed with PBS, digested by 10× TrypLE selected enzyme (Cat# A1217701; GIBCO), diluted 5× in PBS with 1 mM EDTA, and subjected to further experiments. To quantitate BC cells eradicated by ADCP, flow cytometry was performed, and gates distinguishing monocytes from BC cells were established using side scatter or anti-CD14 (Cat# 367116; BioLegend) staining and DiL red fluorescence.

NK and T cell proliferation assay

Autologous NK cells labeled with CTDR were cultured alone or co-cultured with macrophages with the indicated treatments (2:1) in complete medium (RPMI-1640 supplemented with 10% FBS) and stimulated with 100 U/mL IL-2 and 50 U/mL IL-15 (Cat# 200-15; PeproTech) for 4 days. The proliferation rate was then evaluated by flow cytometry for Ki-67 staining (Cat# 350503; BioLegend). In some experiments, 5 μg/mL anti-human B7-H4 neutralizing Ab (eBioscience) or 5 μg/mL mouse IgG2b control (Cat# 400301; BioLegend) was added to the co-culture.

For the T cell proliferation assay, autologous $CD8^+$ T cells were labeled with 0.5 μM CFSE (Cat# C34554; Thermo Fisher Scientific) for 15 min at room temperature and incubated with mature dendritic cells (DCs; 5:1) and the indicated labeled macrophages (2:1) in RPMI-1640 medium supplemented with 5 μg/mL IL-12, 25 mM HEPES, 4 mM L-glutamine, 25 μM 2-mercaptoethanol, and 10% FBS. Proliferation of $CD8^+$ T cells was measured by CFSE staining and flow cytometry after 4 days. In some experiments, 5 μg/mL anti-human B7-H4 neutralizing Ab or 5 μg/mL mouse IgG2b control (Cat# 400301; BioLegend) was added to the co-culture.

ADCC in NK cells

Autologous NK cells labeled with CTDR were cultured alone or co-cultured with the indicated macrophages (2:1) for 48 h. In some experiments, 5 μg/mL anti-human B7-H4 neutralizing Ab or 5 μg/mL mouse IgG2b control was added to the co-culture. Macrophages were then depleted using a CD14 isolation kit (Cat# 130-050-201; Miltenyi Biotec). For monocyte-derived-DC–NK co-culture, NK cells were retrieved using CD56 microbeads (Cat# 130-050-401; Miltenyi Biotec) and co-cultured with $HER2^+$ BC cells pre-stained with CMFDA (10:1) in the presence of 1 μg/mL trastuzumab for 8 h. The cells were then dyed with propidium iodide (PI; 1:300; Cat# 00-6990; eBioscience) and analyzed by flow cytometry. $CMFDA^+PI^+$ cells were designated as killed BC cells. Perforin (Cat# 308106; BioLegend) and granzyme B (Cat# 515403; BioLegend) in $CMFDA^-$ or $CTDR^+$ NK cells were evaluated by surface or intracellular staining and flow cytometry.

Phagocytosis of Escherichia coli particles

Macrophages were plated in black 96-well μClear plates (Greiner Bio-One GmbH, Solingen, Germany). After preincubation for 24 h in DMEM, 10% LPDS, and 25 mM glucose, cells were incubated in DMEM, 10% LPDS, and 0, 6, or 25 mM glucose for 1 and 8 h, respectively. After washing the cells, they were incubated with 100 μL of fluorescein-labeled *E. coli* BioParticles® (Vybrant™ Phagocytosis Assay, Molecular Probes, Invitrogen), suspended in Hanks' balanced salt solution, for 2 h. Subsequently, the suspension was removed and 100 μL of trypan blue suspension was added for 1 min to quench the extracellular probe. After aspiration of trypan blue from the experimental and control wells, fluorescence was measured at 484 nm (excitation) and 535 nm (emission) on a Victor 1420 multilabel counter (PerkinElmer Life Sciences). Phagocytosis was normalized to the protein content in each well.

Cytotoxicity of tumor-specific CD8⁺ T cells

Tumor-specific CD8⁺ T cells generated as described were labeled with CTDR and cultured in the presence or absence of macrophages with the indicated treatments (2:1) for 48 h. In some experiments, 5 μg/mL anti-human B7-H4 neutralizing Ab or 5 μg/mL IgG2b control was added to the co-culture. CD8⁺ T cells were then collected using a CD8 isolation kit (Cat# 130-094-156; Miltenyi Biotec) and mixed with target tumor cells pre-stained with CMFDA (10:1) for 18 h. The cells were then dyed with PI (1:300; Cat# 00-6990; eBioscience) and analyzed by flow cytometry. CMFDA⁺PI⁺ cells were designated as killed BC cells. Perforin (Cat# 308106; BioLegend) and granzyme B (Cat# 515403; BioLegend) CD8⁺ T cells were evaluated by intracellular staining and flow cytometry.

IFN-γ expression in tumor-specific CD4⁺ T cells

Tumor-specific CD4⁺ T cells generated as described were cultured in the presence or absence of macrophages with the indicated treatments (2:1) for 48 h. In some experiments, 5 μg/mL anti-human B7-H4 neutralizing Ab or 5 μg/mL IgG2b control was added to the co-culture. CD4⁺ T cells were then collected by CD4 microbeads (Cat# 130-045-101; Miltenyi Biotec) and mixed with BT-474 cells in the presence or absence of trastuzumab for 24 h. The cells were then stained with anti-CD4 (Cat# 317428; BioLegend) and anti-IFN-γ (Cat# 554700; BD Biosciences) and analyzed by flow cytometry.

Statistical analyses

Statistical analyses were performed using Prism 6.0 software (Macintosh version; GraphPad Software, La Jolla, CA, USA), and data were expressed as the mean þ standard error of the mean (SEM) unless noted otherwise. Differences in the median survival time of mice were determined by Kaplan–Meier survival plots and log-rank tests. The Wilcoxon rank sum test was used for independent samples for analysis of significance, and a $P < 0.05$ was considered significant.

Results

Trastuzumab-opsonized HER2⁺ BC cells undergo phagocytosis by macrophages

We tested whether trastuzumab can mediate cancer cell phagocytosis using BMMs, human macrophages, or a murine macrophage cell line (RAW264.7) as effector cells and HER2⁺ BC cells (MM3MG-HER2Δ16 or SKBR3) as target cells. To investigate whether trastuzumab can induce ADCP of BC cells in macrophages, we labeled HER2⁺ BC cell lines with CTDR and co-cultured them with CMFDA-labeled macrophages for 24 h in the presence or absence of trastuzumab, murine 4D5 mAb trastuzumab (4D5-IgG2A), or their control isotype IgG, respectively. We demonstrated that trastuzumab and 4D5 but not the IgG control increased the proportion of macrophages positive for both dyes in a dose-dependent manner (Fig. 1A and B), indicating trastuzumab-induced phagocytosis of HER2⁺ BC cells by macrophages.

To investigate whether a different activation status of macrophages affects the phagocytotic killing of Ab-opsonized cancer cells, we obtained M1 and M2 macrophages, as well as Mcm macrophages. M1 macrophages exhibited the most potent phagocytosis of HER2⁺ BC cells in the presence of trastuzumab among the tested groups, and both BMMs and M1 macrophages showed significantly more phagocytosis in the presence of trastuzumab relative to that in the presence of the isotype Ab control. However, M2 and Mcm macrophages showed no significant increase in ADCP activity in the presence of trastuzumab relative to that in the presence of the control Ab (Fig. 1C), suggesting that macrophage-activation status affects ADCP activity.

Using transformed MM3MG-HER2Δ16 as a model for HER2-driven BC growth *in vivo*, we then implanted MM3MG-HER2Δ16 cells in the mammary fat pad of immunocompetent BALB/c mice. Tumor-bearing mice were treated with 4D5-IgG2A or clinical-grade trastuzumab to determine whether they could modify the tumor microenvironment. We found that both 4D5-IgG2A and trastuzumab significantly increased macrophage levels (Fig. 1D and E) but had less of an effect on other immune infiltrates, such as NK cells and T cells (Fig. S1A–C).

ADCP in macrophages influences ADCC in NK and T cells

To address whether ADCP in macrophages influence ADCC in NK cells, macrophages were pre-incubated with HER2⁺ BC cells in the presence or absence of trastuzumab for 24 h and then co-cultured with autologous NK cells. As expected, treatment with trastuzumab triggered ADCC by markedly increasing perforin and granzyme B production in and the tumoricidal effects of NK cells (Fig. 2A). Importantly, we observed that macrophages pre-incubated with HER2⁺ BC cells in the presence of trastuzumab (ADCP macrophages) but not untreated macrophages (MΦ) or tumor co-cultured (TC) macrophages without trastuzumab significantly inhibited NK cell proliferation and NK cell-mediated ADCC when co-cultured with HER2⁺ BC cells in the presence of trastuzumab (Fig. 2A), indicating that ADCC suppression by macrophages is ADCP dependent. To confirm this, we inhibited phagocytosis with latrunculin A, a cytochalasin that inhibits actin polymerization, or blocked the three FcγRs with a neutralizing Ab cocktail. Unsurprisingly, inhibition of phagocytosis reversed the observed suppression of NK cell proliferation and ADCC against tumor cells by macrophages (Fig. 2B).

Because adaptive immunity via both CD8⁺ and CD4⁺ T cells is also essential for the therapeutic effects of Abs [28], we determined whether ADCP macrophages can also influence the functions of tumor-specific T cells. We observed that ADCP macrophages dramatically inhibited the proliferation of, production of perforin and granzyme B in, and tumoricidal effects of tumor-specific CD8⁺ T cells (Fig. S2A), as well as the IFN-γ levels in tumor-specific CD4⁺ T cells (Fig. S2B). These data suggested that macrophages that have undergone ADCP are immunosuppressive and inhibit the antitumor functions of NK cells and tumor-specific T cells.

To distinguish whether phagocytosis *per se* or phagocytosis of HER2⁺ breast cancer cells is responsible for the immunosuppressive effect, macrophages were pre-incubated with Lumina A BC cells MCF-7, HER2⁺ BC cells BT-474, BT-474 cells with genetically eliminated HER2, or fluorescein-labeled *E. coli* BioParticles® (Vybrant™ᴹ Phagocytosis Assay, Molecular Probes, Invitrogen) in the presence of trastuzumab for 24 h and

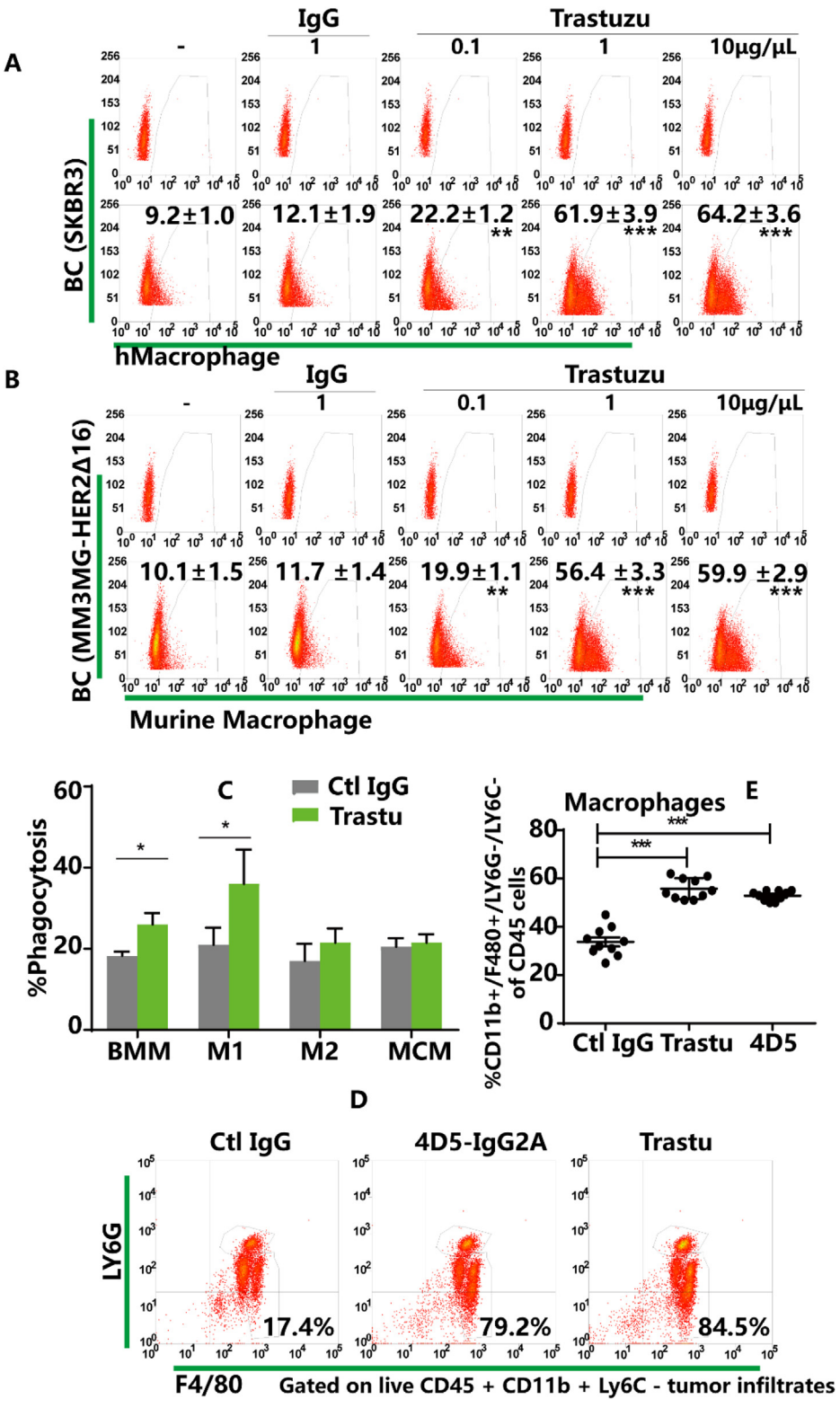

Fig. 1. Trastuzumab-mediated phagocytosis of BC cells by macrophages. (A and B) BMMs (left panel) or RAW264.7 cells (right panel) labeled with CMFDA were co-incubated with human BC cells or murine MM3MG-HER2Δ16 cells labeled with CTDR along with the indicated dose of trastuzumab, murine 4D5 mAb, or control IgG (5 mg/mL) for 24 h. Double-positive (indicating phagocytized cancer cells by macrophages) cells are boxed in the flow dot plot. A representative flow dot plot is shown for each condition. Numerical values denote the mean þ SEM percentage of positive cells among all macrophage ($CMFDA^+$) populations ($n = 5$). $^{**}P < 0.01$, $^{***}P < 0.001$ compared to the untreated group and according to Student's t test. (C) Phagocytosis (%) by different types of macrophages in the presence of trastuzumab or isotype IgG. SDs are indicated by arrow bars, and experiments were repeated three times independently. $^{*}P < 0.05$. (D) MM3MG cells expressing human HER2Δ16 were implanted into the mammary fat pads (1×10^6 cells) of BALB/c mice, and trastuzumab (human IgG1) or 4D5 (mouse IgG2A) was administered ($n = 8$–10). Tumors >1000 mm^3 volume were processed into single-cell suspensions, and (E) macrophages (% $CD11b^+$ $F4/80^+$ $LY6G^-$ $LY6C^-$ among $CD45^+$ cells) were analyzed by FACS and quantified (graphs, right) ($n = 3$).

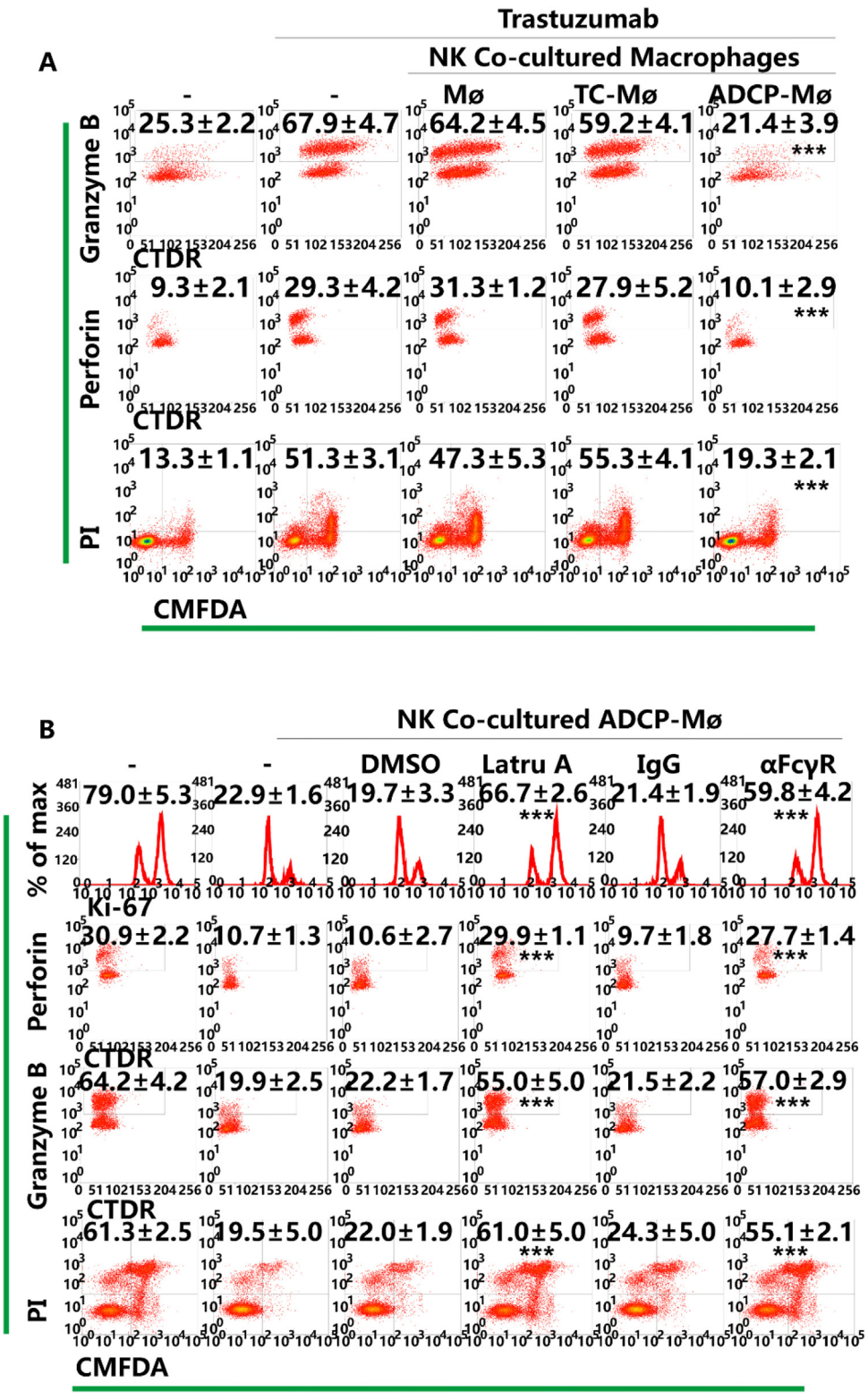

Fig. 2. Macrophages that have undergone ADCP are immunosuppressive. (A) NK cells were cultured alone or co-cultured with the indicated macrophages, and their IL-stimulated proliferation was evaluated by Ki-67 staining. Numerical values denote the mean þ SEM percentage of Ki-67$^+$ cells (n = 5). ***P < 0.001 compared with NK cells cultured alone and according to Student's t test. NK cells co-cultured with the indicated macrophages were labeled with CTDR and co-incubated with HER2$^+$ SKBR3 cells labeled with CMFDA and in the presence or absence of trastuzumab for 12 h. NK cells were stained for intracellular granzyme B or perforin, and dead BC cells were assessed by PI uptake. (B) Latrunculin A or a neutralizing Ab cocktail against activating FcgRs (aFcgRs) were added during ADCP induction. The retrieved macrophages were co-cultured with autologous NK cells, whose proliferation, expression of perforin and granzyme B, and trastuzumab-mediated SKBR3 cell killing were evaluated. Representative plots are shown. Values represent the mean þ SEM (n = 5). ***P < 0.001 as compared with the group cultured alone and according to Student's t test.

then co-cultured with autologous natural killer (NK) cells. Treatment with trastuzumab triggered antibody-dependent cellular cytotoxicity (ADCC) by markedly increasing the production of perforin and granzyme B, and tumoricidal effects of NK cells as shown in Fig. 2A. Impressively, macrophages pre-incubated with HER2$^+$ tumor cells in the presence of trastuzumab (ADCP macrophages), but not those pre-incubated with Lumina A BC cells (MCF-7) or bacteria (*E. coli* BioParticles) inhibited NK cell proliferation and suppressed NK cell-mediated ADCC in the presence of trastuzumab. Further, pre-incubation of macrophages with BT-474 cells whose HER2 was genetically eliminated even in the presence of trastuzumab did not have any suppressive effect on NK cell-mediated ADCC against tumor cells (Fig. S2C), suggesting that this was ADCP macrophage-specific.

B7-H4 levels increase in macrophages following Trastuzumab-dependent phagocytosis of BC cells

We then investigated whether strategies to enhance ADCP might be synergistic with trastuzumab therapies. Because previous studies demonstrated that B7-H4 expression identifies a suppressive macrophage population, we explored whether targeting this molecule would enhance HER2 mAb ADCP. We first documented the elevated expression of B7-H4 in *in vitro* ADCP macrophages (Fig. 3A). To further investigate whether human B7-H4 limits the ADCP effects of trastuzumab against HER2$^+$ BC cells, B7-H4 expression was either blocked by a neutralizing Ab or shRNA KD in ADCP macrophages. Flow cytometric evaluation revealed that neutralization of B7-H4 increased BC cell susceptibility to trastuzumab-mediated ADCP (Fig. 3B). Similarly, BC cell phagocytosis by B7-H4 KD macrophages in the presence of trastuzumab increased significantly relative to that by parental macrophages (Fig. 3C). These results suggested that loss of B7-H4 could unleash the full potential of trastuzumab efficacy by altering macrophage activation.

To determine the contribution of this molecule to ADCP and ADCC *in vitro*, we added the anti-B7-H4 Ab to the co-cultures of macrophages and NK cells, finding that B7-H4 neutralization significantly alleviated the suppressive effects of ADCP macrophages on NK cell proliferation and ADCC (Fig. 3D). Additionally, ADCP-mediated suppression of the tumoricidal effects of tumor-specific CD8$^+$ T cells was consistently reversed by B7-H4 inhibition (Fig. 3E).

We then evaluated the effect of B7-H4 expression on tumor growth and HER2 mAb therapy *in vivo*. We implanted a PDX from a surgical HER2$^+$ BC specimen with or without trastuzumab neoadjuvant therapy into NSG mice engrafted with monocytes from the corresponding patient, followed by subsequent therapy with clinical-grade trastuzumab. For the neoadjuvant PDXs, we observed a strong effect from trastuzumab treatment that was significantly enhanced in the presence of B7-H4-KD monocytes (Fig. 3F), resulting in tumors being substantially eliminated and elevated macrophage number (Fig. S3A and B). For the same PDXs, in the presence of B7-H4-overexpressing monocytes (Fig. 3G), we observed increased PDX resistance to trastuzumab therapy (Fig. S3C) and attenuated macrophage number (Fig. S3D). These results indicated that the immunosuppressive effects of macrophages following trastuzumab-dependent BC phagocytosis were abrogated by relieving the B7-H4 checkpoint.

B7-H4 blockade increases the therapeutic efficacy of trastuzumab in a murine model of HER2$^+$ BC and augments macrophage phagocytosis

To further explore whether immune-checkpoint inhibitors (ICIs) can improve tumor response to therapeutic mAbs, we combined the 4D5-IgG2A mAb with the B7-H4 neutralizing Ab in immunocompetent mice harboring MM3MG-HER2Δ16 tumors. Although 4D5-IgG2A and B7-H4 neutralization both showed therapeutic efficacy, addition of the B7-H4 neutralizing Ab significantly improved the response of human HER2$^+$ tumors to 4D5 (Fig. 4A) and increased macrophage number (Fig. 4B).

To directly demonstrate tumor ADCP by endogenous macrophages in the tumor microenvironment, we labeled MM3MG-HER2Δ16 tumor cells with DiD dye, a carbocyanine membrane-binding probe, prior to implantation in order to detect phagocytosis of labeled target cells *in vivo* [29]. When the tumors were palpable, we treated the animals with either 4D5-IgG2A alone or both 4D5-IgG2A and the B7-H4 neutralizing Ab. FACS analysis showed increased phagocytosis of labeled BC cells by macrophages in 4D5-IgG2A-treated animals, directly demonstrating that 4D5-IgG2A treatment promotes ADCP of HER2$^+$ tumor cells *in vivo*. However, addition of the B7-H4 neutralizing Ab increased ADCP of labeled cells by macrophages (Fig. 4C and D). These findings demonstrated that the HER2 mAb stimulated ADCP by endogenous macrophages against HER2$^+$ BC, which was synergistically enhanced by B7-H4 neutralization.

B7-H4 blockade synergizes trastuzumab-mediated therapeutic activity in a humanized HER2$^+$ BC mouse model

Having demonstrated trastuzumab efficacy in a murine model of HER2$^+$ BC, we extended the analysis using humanized NSG mice bearing PDXs, as previously described [15], with animals harboring palpable breast tumors enrolled in a specific treatment group. We demonstrated that trastuzumab monotherapy significantly increased survival time and delayed tumor growth, whereas treatment with the B7-H4 neutralizing Ab alone showed a less significant effect relative to the control group. Interestingly, animals receiving both agents showed prolonged survival rates and delayed tumor growth and were substantially more susceptible to trastuzumab-mediated inhibition of tumor growth (Fig. 5A and B), suggesting that this combined therapy may be efficacious in HER2$^+$ BCs.

To determine whether these therapies alter levels of immune infiltrates, we analyzed the composition of the tumor microenvironment. Evaluation of the effects of combined treatment with mAbs and ICIs on the immune microenvironment revealed an increase in macrophage number following trastuzumab monotherapy, whereas the combined therapy showed an even higher increase (Fig. 5C). We then examined NK and CD8+ T cell infiltration into tumor grafts using IHC. The results showed that administration of trastuzumab or the B7-H4 neutralizing Ab alone only slightly increased the number of tumor-infiltrating NK and CD8+ T cells, whereas combined trastuzumab and B7-H4 Ab treatment substantially increased the number of NK and CD8+ T cells in the tumors. (Fig. 5C–F). These results suggested that combined application of ICIs improved the efficacy of therapeutic antibodies by enhancing antitumor immunity.

Human B7-H4 gene expression is a prognostic factor and limits the therapeutic efficacy of trastuzumab in HER2$^+$ BC

We then determined whether trastuzumab-mediated ADCP activity occurs in human HER2$^+$ BC and whether B7-H4 limits its antitumor efficacy. We examined immune cell infiltration in paired pretreatment biopsies and post-treatment resected samples from BC patients who had received neoadjuvant trastuzumab-based therapy. We observed only modest levels of *B7-H4* expression in stromal cells in HER2$^+$ BC biopsies before neoadjuvant therapy. However, tumor-infiltrating macrophages expressed considerably higher levels of *B7-H4* after trastuzumab-containing neoadjuvant therapy. Nevertheless, HER2$^+$ patients who had received neoadjuvant chemotherapy without trastuzumab did not exhibit enhanced *B7-H4* expression in macrophages in post-treatment samples (Fig. 6A and B). Moreover, the number of B7-H4$^+$ tumor-infiltrating

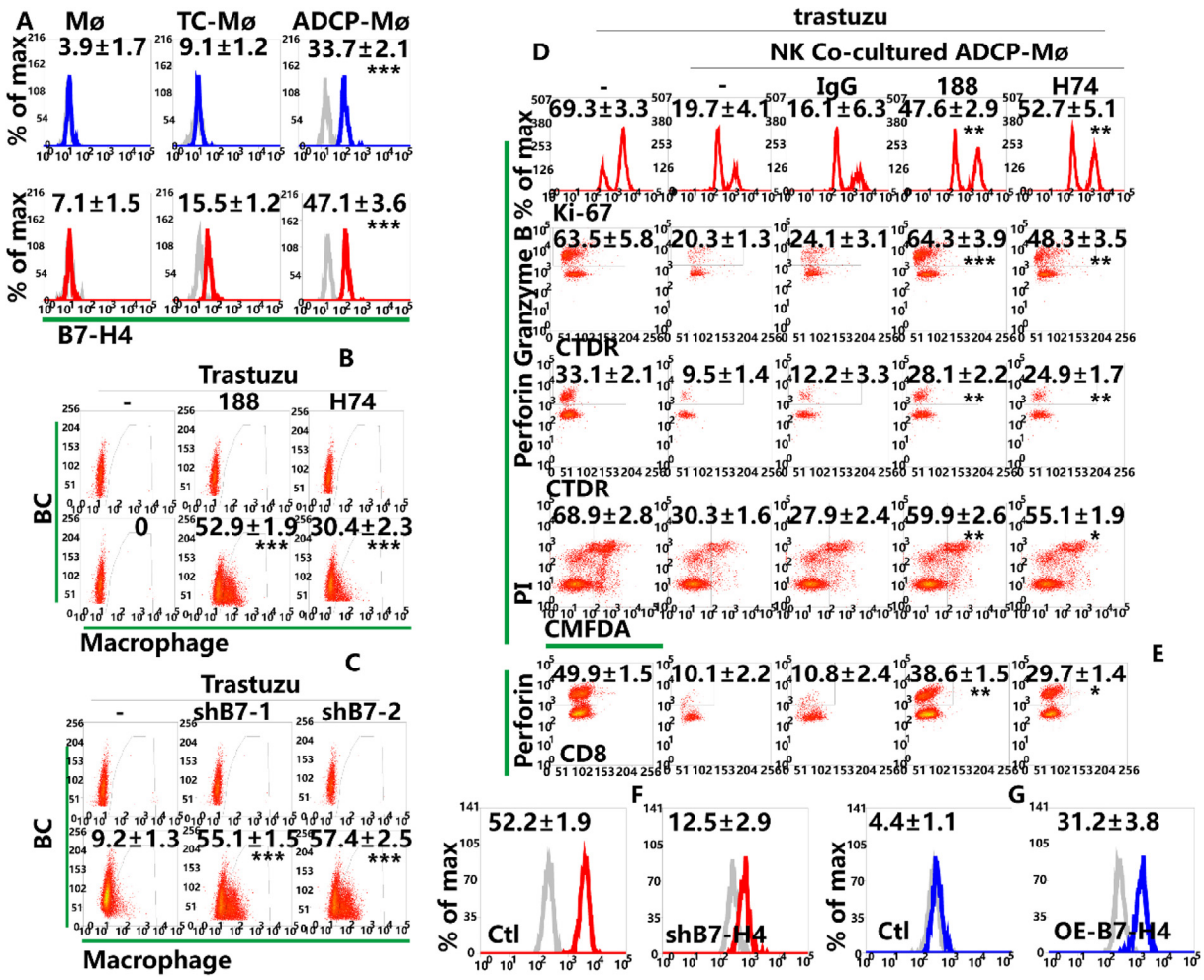

Fig. 3. B7-H4 limits trastuzumab-mediated ADCP of HER2$^+$ human BC cells. (A) Human macrophages were cultured alone (MΦ) or co-cultured with BC cells without (TC-MΦ) or with trastuzumab (ADCP-MΦ), and B7-H4 expression was evaluated by flow cytometry. (B) Neutralizing antibodies against B7-H4 were added to the macrophage–BC cell co-culture system in the presence or absence of trastuzumab. Double-positive cells represent macrophages that engulfed tumor cells. Numerical values denote the mean þ SEM percentage of positive cells among all macrophage (CMFDA+) populations (n = 5). ***P < 0.001 compared with the control according to Student's t test. (C) WT or B7-H4 KD ADCP-MΦ labeled with CMFDA were co-incubated with SKBR3 cells labeled with CTDR in the presence of trastuzumab. Numerical values represent the mean þ SEM percentage of positive cells among all macrophage (CMFDA+) populations (n = 5). P < 0.001 compared with WT macrophages co-cultured with SKBR3 cells in the presence of trastuzumab according to Student's t test. (D) NK cells were co-cultured with macrophages following trastuzumab-dependent BC cell phagocytosis in the presence or absence of a B7-H4 neutralizing Ab. NK cell proliferation, expression of perforin and granzyme B, and BC cell killing were evaluated by flow cytometry. (E) Macrophages performing trastuzumab-mediated SKBR3 cell phagocytosis were co-cultured with tumor-specific CD8$^+$ T cells in the presence or absence of a B7-H4 neutralizing Ab, and perforin expression in CD8$^+$ T cells was evaluated. Values represent the mean þ SEM (n = 5). *P < 0.05, **P < 0.01, ***P < 0.001 according to Student's t test. **(F)** Flow cytometric confirmations of B7-H4 KD in macrophages. (G) Flow cytometric confirmation of B7-H4 overexpression in monocytes. All data represent the mean þ SEM. *P < 0.05, ***P < 0.001, ****P < 0.0001.

macrophages was associated with poor response to trastuzumab-containing neoadjuvant therapy (Fig. 6C) and negatively correlated with infiltration of NK and CD8$^+$ T cells (Fig. 6B and D). Collectively, data from patients suggested that *B7-H4* expression was elevated in macrophages following trastuzumab therapy and inhibited the antitumor function of NK and CD8$^+$ T cells.

Discussion

Stroma inhibits infiltration and activation of tumor T cells [30–32]. However, it is poorly understood how each cellular component in tumor stroma contributes to tumor immunopathogenesis. After several decades of neglect, immune suppressor cells are once again an area of active research interest. The best studied immune suppressor population is the well-known yet still relatively newly described CD4$^+$CD25$^+$ Treg cells [33–35], which disable TAA-specific T cell immunity [36,37].

Anti-HER2/neu antibody therapy is reported to mediate tumor regression by interrupting oncogenic signals and/or inducing FcR-mediated cytotoxicity [1,38,39]. Here, we demonstrate that the mechanisms of tumor regression by this therapy also require the adaptive immune response. In this study using multiple models of human HER2-expressing BC and using the murine version of trastuzumab with the functionally equivalent mouse isotype (4D5-IgG2A), we demonstrate that macrophages are the major effectors carrying out the antitumor immunity of trastuzumab therapy through ADCP. Although it is thought that many therapeutic mAbs for human malignancies, including trastuzumab, function primarily through NK cell-mediated ADCC [40–42], several lines

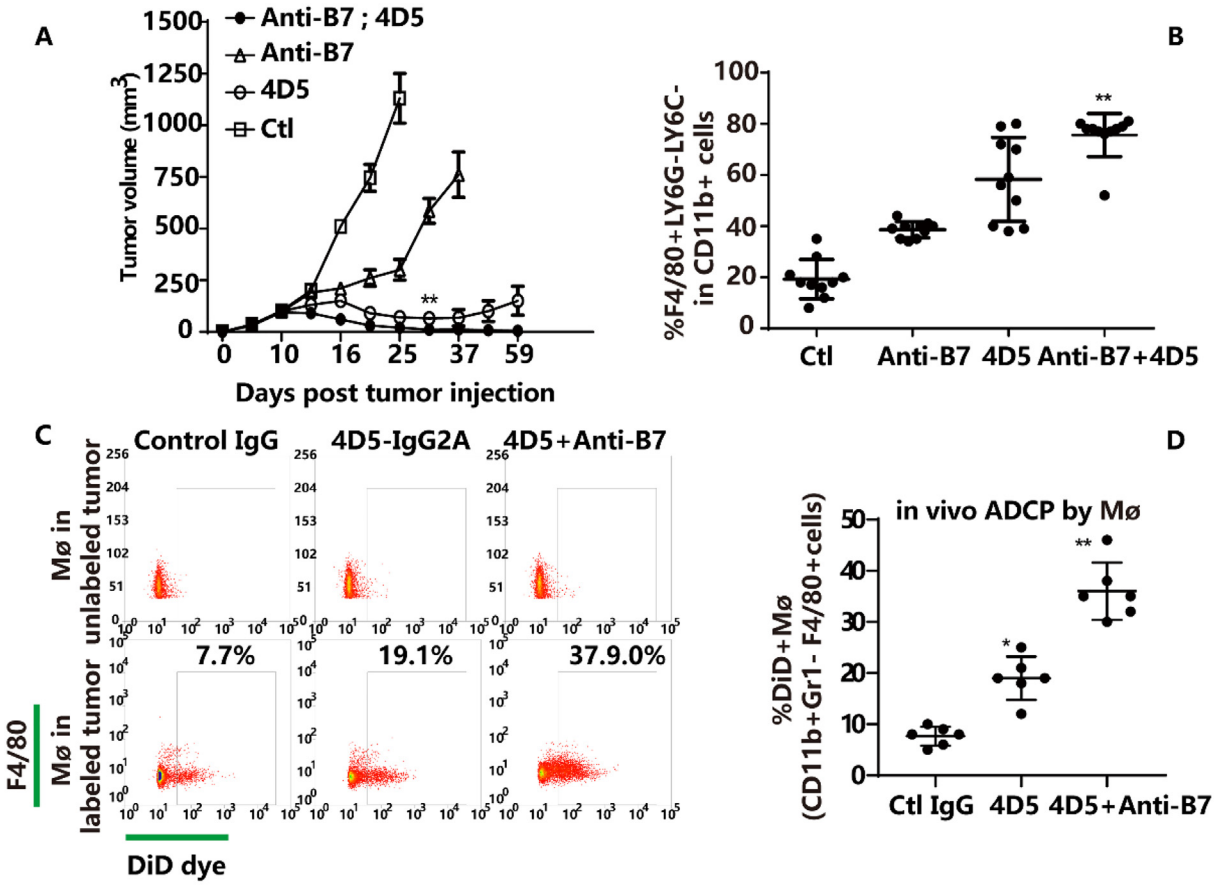

Fig. 4. B7-H4 neutralization enhances trastuzumab efficacy in immunocompetent mice harboring BC tumors. (A) Tumor-growth experiment involving a B7-H4 neutralizing Ab (100 μg/mouse) alone or combined with 4D5-IgG2a (200 μg). (B) Macrophage populations were analyzed by FACS after tumor volume reached >1000 mm^3. Data represent the mean þ SEM (n = 8–10). (C and D) *In vivo* ADCP experiment. MM3MG-HER2Δ16 cells were labeled with Vybrant DiD dye and implanted (1×10^6 cells) into the mammary fat pads of BALB/c mice. After the TV reached ∼1000 mm^3, mice were treated with a control Ab, 4D5-IgG2A (200 μg), or 4D5-IgG2A in combination with the B7-H4 neutralizing Ab (100 μg). Tumors were harvested, and tumor-phagocytic macrophages were quantified by FACS (D). Representative FACS plots and graphical summary showing the frequency of macrophages ($CD11b^+F4/80^+LY6G^-LY6C^-$) that have phagocytosed DiD-labeled BC cells.

of evidence from this study indicate that the therapeutic effect of immune checkpoint antibody alone or in combination with trastuzumab is mediated primarily through macrophage phagocytosis. First, the depletion of macrophages but not neutrophils had a significant negative effect on trastuzumab efficacy; second, trastuzumab treatment greatly and consistently increased macrophage frequency; third, the therapeutic effect of combination antibody treatment in a BC xenotransplant model using complement and NK cell-deficient NSG mice was similar to complement and NK cell-competent SCID mice, suggesting that macrophages alone are sufficient to mediate the therapeutic effect.

We further demonstrated that trastuzumab induces macrophages to have a highly phagocytic and antitumor phenotype, and also produces an immunosuppressive phenotype related to tumor-associated macrophages following prolonged tumor phagocytosis. Therefore, we demonstrated the ability of trastuzumab to elicit ADCP, while trastuzumab-mediated ADCP triggers macrophage immunosuppression in $HER2^+$ BC that limits macrophage ADCP. This specific recruitment of macrophages represents a mechanism by which tumors may foster immune privilege. Other studies have demonstrated that cellular phagocytosis over time influences macrophage phenotype, causing a switch from a proinflammatory to a growth-promoting, reparative phenotype [43,44]. Therefore, our study advances the understanding of macrophage plasticity by uncovering a dual role of ADCP in macrophages: eliminating tumors by engulfing BC cells while causing a concomitant undesired effect by upregulating immunosuppressive checkpoints. We thus provide insight into the utility of macrophages as potent mediators of antitumor immunity that can be further exploited. It is necessary to monitor immune-checkpoint expression during Ab treatment. We also provide a rationale for using ICIs in BCs treated with a therapeutic Abs.

In this study, we report a novel suppressive cell population in patients with BCs, namely $B7\text{-}H4^+$ macrophages. The notion that tumor macrophage B7-H4 signals contribute to immunopathology and ADCP resistance is supported by several lines of evidence. First, $B7\text{-}H4^+$ tumor macrophages are significantly more suppressive than $B7\text{-}H4^-$ counterparts. Second, blocking B7-H4 on tumor-conditioned macrophages disables their suppressive capacity. Third, forced B7-H4 expression renders normal macrophages suppressive. Fourth, blocking B7-H1 and inhibiting iNOS and arginase have minor effects on $B7\text{-}H4^+$ macrophage-mediated T cell suppression [43,45–49]. This conclusion is also supported by the enhanced effects observed between trastuzumab and B7-H4 blockade in augmenting ADCP and antitumor effects in our study. Further, ADCP was proposed as the ultimate mechanism for tumor clearance. These data indicate that the suppressive potency of $B7\text{-}H4^+$ macrophages is similar to that of $CD4^+$ Treg cells [50]. We also observed a similar regulatory mechanism for B7-H4 expression on myeloid dendritic cells [51]. Recent observations also suggest a mechanistic link between $B7\text{-}H4^+$ APCs, including

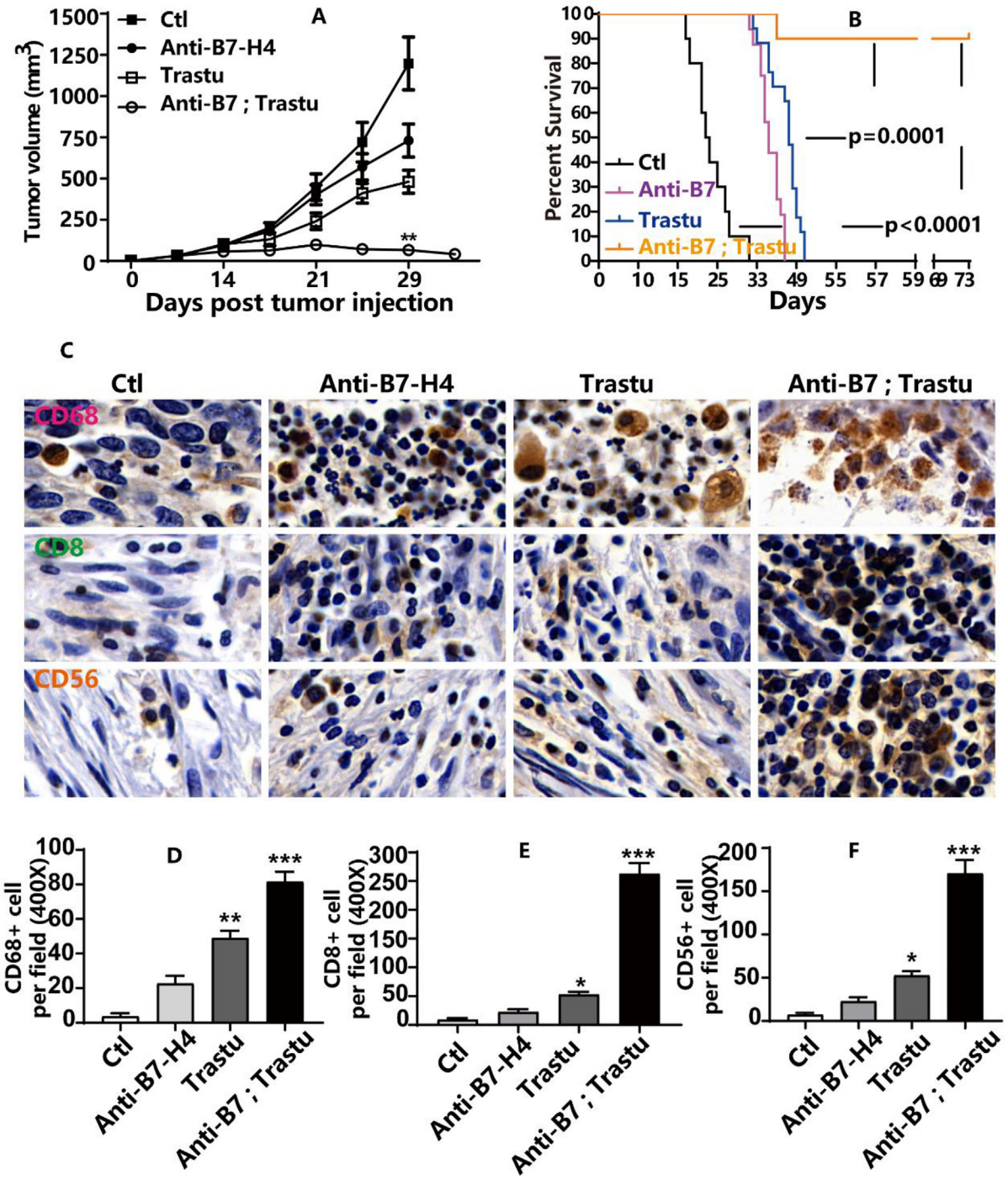

Fig. 5. B7-H4 blockade enhanced trastuzumab efficacy in a humanized HER2$^+$ BC mouse model. (A) Four treatment arms were established: control IgG (200 μg weekly; $n = 15$); B7-H4 blockade (100 μg weekly; $n = 15$); trastuzumab (200 μg weekly; $n = 15$); and trastuzumab combined with B7-H4 neutralizing Ab ($n = 15$). Individual animals were consecutively enrolled into a specific treatment arm as soon as palpable BCs were detected (~200 mm^3). The total tumor burden per mouse is shown. Animals were euthanized when their total TV reached >2000 mm^3. (B) Survival of mice in each treatment arm. Time of start was on the day of palpable tumor detection and treatment enrollment. The log rank (Mantel–Cox) test was used for survival analysis. $^{****}P < 0.0001$, treatment vs. control group; $\#\#P < 0.01$, difference observed between the trastuzumab and trastuzumab + anti-B7-H4 groups. (C) Humanized mice bearing palpable xenografts were administrated with the indicated treatments. Representative IHC images of immune cell infiltration are shown (scale bar, 50 μm). (D–F) Immune cell populations per high-power microscope field in tumor tissues ($n = 5$ mice/group).$^*P < 0.05$; $^{**}P < 0.001$;$^{***}P < 0.0001$ according to a paired t test.

macrophages and CD4$^+$ Treg cells [36,51]. In fact, CD4$^+$ Treg cells stimulate APC B7-H4 expression and enable APC suppressive activity through B7-H4 induction [51]. B7-H4$^+$ tumor macrophages significantly outnumber CD4$^+$ Treg cells in solid tumor mass. Thus, their contribution to tumor immune evasion is likely substantial. These further support our hypothesis that total tumor macrophage-mediated immunosuppression

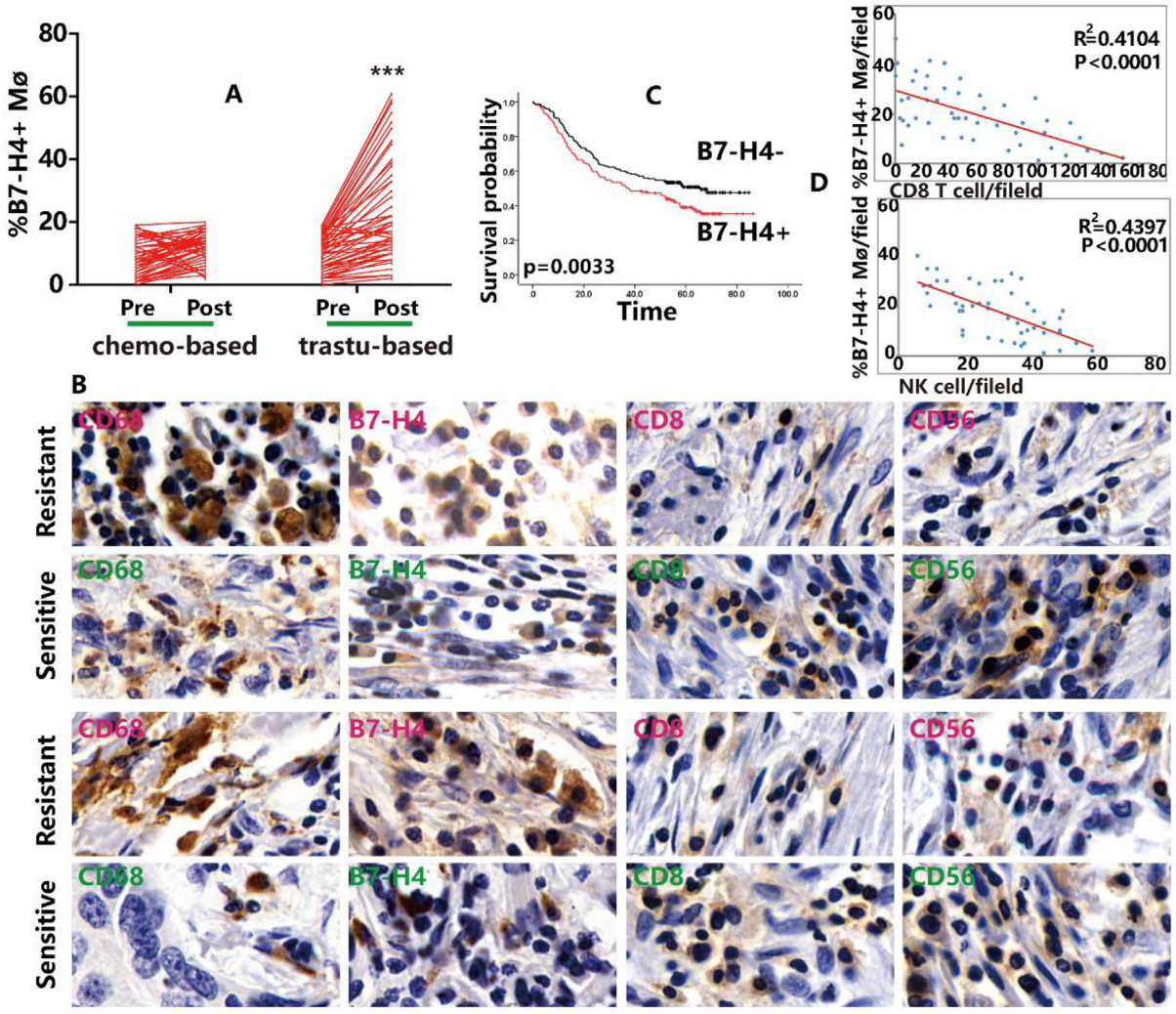

Fig. 6. Human B7-H4 gene expression is a prognostic factor in HER2$^+$ BCs and limits the therapeutic efficacy of trastuzumab. (A) Quantitation of CD68 and B7-H4 IHC staining in paired samples of HER2$^+$ BC patients before and after neoadjuvant trastuzumab therapy or neoadjuvant chemotherapy without trastuzumab ($n = 50$ in the trastuzumab group; $n = 58$ in the chemotherapy group). ***$P < 0.001$, Student's t test. (B) Representative images of CD68, B7-H4, CD8, and CD56 in serial sections of the paired clinical samples from HER2$^+$ breast cancer patients before and after neoadjuvant therapy. Scale bar, 50 μm. (C) Kaplan–Meier survival curve for BC patient data and stratified into low and high groups based on the average expression of *B7-H4* in BC-infiltrating macrophages. (D) Correlation of infiltrations (number per view field) of B7-H4$^+$ macrophages and NK cells or CD8$^+$ T cells in clinical samples from BC patients after neoadjuvant trastuzumab therapy [$n = 50$, Pearson's correlation coefficient (R and P are shown)].

predominantly comes from the B7-H4$^+$ tumor macrophage subset. Therefore, the BC microenvironment presents an overwhelming arsenal of actively tolerizing mechanisms, including an imbalance of plasmacytoid versus myeloid DCs [52], costimulatory molecules versus coinhibitory molecules [53,54], and tumor associated macrophages versus effector T cells [50].

In order to investigate whether anti-B7-H4 plus anti-HER2/neu antibody is always better than antibody alone, we report two mouse models with different background for BC in which orthotopic implantation of cells from a murine harboring HER2$^+$ breast cancer and a HER2$^+$ BC patient gives rise to robust BC engraftment. We found mice to regress established tumors efficiently after anti-neu antibody treatment. We also expected the combination of anti-B7-H4 at this time dose synergized with anti-neu antibody to control the established tumors. However, this antibody treatment seemed to have a very limited impact on the growth of tumors in mice (Fig. 4A), since trastuzumab had strongly inhibited tumor growth by more than 80% via interruption of oncogenic signals. Thus, as shown in Fig. 4A, although addition of the B7-H4 neutralizing Ab improved the response of HER2$^+$ BC tumors to 4D5 at some time points on the graph, this improvement is not very impressive. Furthermore, we observed that, a single dose of trastuzumab only enabled a partial reduction in tumor burden that rebounded back to baseline levels with no further reduction observed in the following days (Fig. 4A). Impressively, mice administered a combination therapy of anti-B7-H4 antibody and trastuzumab demonstrated complete elimination of BC, with 90% (9 out of 10 mice) treated mice having no measurable mass, 4 weeks after the end of therapy; moreover, all showed no evidence of tumor growth, remained relapse free, and were alive at over 100 days after tumor engraftment. Out of 9 mice achieving a complete remission, 9 remained relapse free whereas one mouse died of non-tumor-related causes (Fig. 4A and 5B).

We speculate that there might be a window of time when trastuzumab may effectively reduce tumor burden without inhibiting antibody-induced immunity; that is, the addition of trastuzumab, while capable of strongly enhancing the reduction of tumor burden, could simultaneously abrogate antibody-initiated immunity leading to decreased resistance and an earlier relapse. The optimal impact of anti-neu antibody treatment on tumor growth, however, likely depends a lot on the amount of antigen presenting cells inside the tumor microenvironment. These data raise an interesting possibility that anti-B7-H4 antibody may transiently break tolerance in mouse models and rejuvenate immunity against HER2/neu$^+$ tumors. The role of B7-H4 blockade in the efficacy of antibody treatment is further supported by the evidence that sequential administration of anti-B7-H4 antibody after anti-HER2/neu may allow the completely remitted mice to be protected from a second tumor challenge with twice the original tumor load or relapse, suggesting that these mice can develop immunologic memory. Therefore, combining this antibody treatment that can break tumor barriers and attract immune cells, may have great impacts on the efficacy of anti-HER2/neu antibody treatment. Due to the nature of immune therapy, anti-B7-H4 had less effect on tumor clearance but synergized with anti-neu antibody to preserve the ability of the host to clear a lethal tumor re-challenge or relapse. Therefore, it was not surprising that B7-H4 targeting did not significantly enhance suppression of the growth of tumors in Fig. 4A but allowed anti-HER2/neu treatment to maintain relapse free and long-term survival as shown in Fig. 5B.

Here, our current findings demonstrate that the anti-neu antibody is very potent in blocking oncogenic signals for tumor elimination. Given the importance of danger signals in initiating immunity, we propose that blocking oncogenic signals by the anti-HER2/neu antibody may be an important initiator of, and positive-feedback loop for, adaptive immunity by supporting the critical role of B7-H4 targeting for reinvigorating immunity. Although anti-B7-H4 fails to regress tumor, it confers a robust protection from tumor re-challenge, a potential problem related to late relapse observed in the clinic once primary tumor is diminished after treatment [55]. Since the treatment of HER2$^+$ tumors with trastuzumab has been available for many years [56], this observation suggests that B7-H4 targeting might be functioning in ADCP-mediated therapeutic resistance. Future experiments using a combination of trastuzumab and anti-B7-H4, analyzing multiple treatment time points, reducing the length of treatment, or combining with other immune-checkpoint blockades could potentially improve tumor-specific cytotoxic infiltration. Although this is an area that needs additional study, our results suggest that strategies to specifically enhance ADCP activity might be critical for overcoming resistance to HER2 mAb therapies by inhibiting tumor growth and potentially enhancing antigen presentation.

Funding

This work was supported in part by grants from the National Natural Science Foundation of China (U1404817 and 81702820 to Xiang Yuan), One thousand Young People Plan of Henan Province (to Xiang Yuan), Project of Science and Technology Department of Henan Province (202102310023 to Xiang Yuan), Project of Henan Health Department (SB201902022 to Xiang Yuan), Young Academic Leaders of Henan University of Science and Technology (to Xiang Yuan), China Postdoctoral Science Foundation (171234 to Xiang Yuan), and Project of Henan Education Department (16A320038 to Xurong Hou).

Disclosure of potential conflicts of interest

The authors have no potential conflicts of interest to disclose.

Acknowledgments

The authors gratefully thank Dr. Chen at the University of Pittsburgh (Pittsburgh, PA, USA) and Dr. Cao at the University of California Los Angeles (Los Angeles, CA, USA), for their help in experimental technologies and for critically editing a draft of this article. Also, we thank Jianqiang Mi and Hongbo Han for their help with pathologic diagnosis of the enrolled patients. This work was supported in part by grants from the National Natural Science Foundation of China (U1404817 and 81702820 to Xiang Yuan), One thousand Young People Plan of Henan Province (to Xiang Yuan), Project of Science and Technology Department of Henan Province (202102310023 to Xiang Yuan), Project of Henan Provincial Department of Health (SB201902022 to Xiang Yuan),Young Academic Leaders of Henan University of Science and Technology (to Xiang Yuan), China Postdoctoral Science Foundation (171234 to Xiang Yuan), and Project of Henan Education Department (16A320038 to Xurong Hou).

Authors contributions

Conception and design: Xiang Yuan, Xiaochen Hu.

Development of methodology: Yiwen Liu, Xiusen Zhang, Dejiu Kong, Di Zhao, Shupei Liu, Jinyu Kong, Yibo Guo, Lingyun Sun, Luoyi Chu.

Acquisition of data (provided animals, acquired and managed patients, provided facilities, etc.): Xiaochen Hu, Xurong Hou, Feng Ren, Ying Zhao, Desheng Zhai.

Analysis and interpretation of data (e.g., statistical analysis, biostatistics, computational analysis): Xiaochen Hu, Yiwen Liu, Xiusen Zhang, Dejiu Kong, Jinyu Kong, Yibo Guo.

Writing, review, and/or revision of the manuscript: Xiang Yuan, Xiaochen Hu.

Administrative, technical, or material support (i.e., reporting or organizing data, constructing databases): Chengbiao Lu, Desheng Zhai.

Study supervision: Xiang Yuan, Xiaochen Hu.

Our study advances the understanding of macrophage plasticity by uncovering a dual role of ADCP in macrophages: eliminating tumors by engulfing BC cells while causing a concomitant undesired effect by upregulating immunosuppressive checkpoints. Anti-B7-H4 antibody may transiently break tolerance in mouse models and rejuvenate immunity against HER2/neu$^+$ tumors to confer a robust protection from tumor re-challenge, a potential problem related to late relapse observed in the clinic once primary tumor is diminished after treatment. We thus provide a rationale for using ICIs in BCs treated with a therapeutic Abs.

Appendix A. Supplementary data

Supplementary data to this article can be found online at https://doi.org/10.1016/j.neo.2020.08.007.

References

1. Slamon DJ, Clark GM, Wong SG, Levin WJ, Ullrich A, McGuire WL. Human breast cancer: correlation of relapse and survival with amplification of the HER-2/neu oncogene. *Science* 1987;**235**:177–82.
2. Braman N, Prasanna P, Whitney J, Singh S, Beig N, Etesami M, Bates DDB, Gallagher K, Bloch BN, Vulchi M, et al. Association of peritumoral radiomics with tumor biology and pathologic response to preoperative targeted therapy for HER2 (ERBB2)-positive breast cancer. *JAMA Netw open* 2019;**2** e192561
3. Di Fiore PP, Pierce JH, Kraus MH, Segatto O, King CR, Aaronson SA. erbB-2 is a potent oncogene when overexpressed in NIH/3T3 cells. *Science* 1987;**237**:178–82.

4. Bianchini G, Gianni L. The immune system and response to HER2-targeted treatment in breast cancer. *Lancet Oncol* 2014;**15**:e58–68.
5. Shak S. Overview of the trastuzumab (Herceptin) anti-HER2 monoclonal antibody clinical program in HER2-overexpressing metastatic breast cancer. Herceptin Multinational Investigator Study Group. *Semin Oncol* 1999;**26**:71–7.
6. Balachandran VP, Cavnar MJ, Zeng S, Bamboat ZM, Ocuin LM, Obaid H, Sorenson EC, Popow R, Ariyan C, Rossi F, et al. Imatinib potentiates antitumor T cell responses in gastrointestinal stromal tumor through the inhibition of Ido. *Nat Med* 2011;**17**:1094–100.
7. Tsao LC, Crosby EJ, Trotter TN, Agarwal P, Hwang BJ, Acharya C, Shuptrine CW, Wang T, Wei J, Yang X, et al. (2019). CD47 blockade augmentation of trastuzumab antitumor efficacy dependent on antibody-dependent cellular phagocytosis JCI Insight 4.
8. Zhu EF, Gai SA, Opel CF, Kwan BH, Surana R, Mihm MC, Kauke MJ, Moynihan KD, Angelini A, Williams RT, et al. Synergistic innate and adaptive immune response to combination immunotherapy with anti-tumor antigen antibodies and extended serum half-life IL-2. *Cancer Cell* 2015;**27**:489–501.
9. Naranjo-Gomez M, Lambour J, Piechaczyk M, Pelegrin M (2018). Neutrophils are essential for induction of vaccine-like effects by antiviral monoclonal antibody immunotherapies, JCI Insight 3.
10. Stagg J, Loi S, Divisekera U, Ngiow SF, Duret H, Yagita H, Teng MW, Smyth MJ. Anti-ErbB-2 mAb therapy requires type I and II interferons and synergizes with anti-PD-1 or anti-CD137 mAb therapy. *PNAS* 2011;**108**:7142–7.
11. Trivedi S, Srivastava RM, Concha-Benavente F, Ferrone S, Garcia-Bates TM, Li J, Ferris RL. Anti-EGFR targeted monoclonal antibody isotype influences antitumor cellular immunity in head and neck cancer patients. *Clin Cancer Res* 2016;**22**:5229–37.
12. Barry WE, Jackson JR, Asuelime GE, Wu HW, Sun J, Wan Z, Malvar J, Sheard MA, Wang L, Seeger RC, et al. Activated natural killer cells in combination with anti-GD2 antibody dinutuximab improve survival of mice after surgical resection of primary neuroblastoma. *Clin Cancer Res* 2019;**25**:325–33.
13. Mantovani A, Longo DL. Macrophage checkpoint blockade in cancer – back to the future. *N Engl J Med* 2018;**379**:1777–9.
14. Zou W, Chen L. Inhibitory B7-family molecules in the tumour microenvironment. *Nat Rev Immunol* 2008;**8**:467–77.
15. Yuan X, Liu Y, Li G, Lan Z, Ma M, Li H, Kong J, Sun J, Hou G, Hou X, et al. (2019). Blockade of immune-checkpoint B7-H4 and lysine demethylase 5B in esophageal squamous cell carcinoma confers protective immunity against P. gingivalis infection, Cancer Immunol Res 7, 1440–1456.
16. Kryczek I, Zou L, Rodriguez P, Zhu G, Wei S, Mottram P, Brumlik M, Cheng T, Curiel T, Myers L, et al. B7–H4 expression identifies a novel suppressive macrophage population in human ovarian carcinoma. *J Exp Med* 2006;**203**:871–81.
17. The official journal of the American Society for Bone and Mineral Research. Issue information-Declaration of Helsink. *J Bone Miner Res* 2017:**32**;BM i -ii.
18. Gao S, Li S, Ma Z, Liang S, Shan T, Zhang M, Zhu X, Zhang P, Liu G, Zhou F, et al. Presence of Porphyromonas gingivalis in esophagus and its association with the clinicopathological characteristics and survival in patients with esophageal cancer. *Infect Agents Cancer* 2016;**11**:3.
19. Yuan X, Wang X, Gu B, Ma Y, Liu Y, Sun M, Kong J, Sun W, Wang H, Zhou F, et al. Directional migration in esophageal squamous cell carcinoma (ESCC) is epigenetically regulated by SET nuclear oncogene, a member of the inhibitor of histone acetyltransferase complex. *Neoplasia* 2017;**19**:868–84.
20. Sun J, Li G, Liu Y, Ma M, Song K, Li H, Zhu D, Tang X, Kong J, Yuan X. Targeting histone deacetylase SIRT1 selectively eradicates EGFR TKI-resistant cancer stem cells via regulation of mitochondrial oxidative phosphorylation in lung adenocarcinoma. *Neoplasia* 2020;**22**:33–46.
21. Yuan X, Liu Y, Kong J, Gu B, Qi Y, Wang X, Sun M, Chen P, Sun W, Wang H, et al. Different frequencies of Porphyromonas gingivalis infection in cancers of the upper digestive tract. *Cancer Lett* 2017;**404**:1–7.
22. Yuan X, Kong J, Ma Z, Li N, Jia R, Liu Y, Zhou F, Zhan Q, Liu G, Gao S. KDM4C, a H3K9me3 histone demethylase, is involved in the maintenance of human ESCC-initiating cells by epigenetically enhancing SOX2 expression. *Neoplasia* 2016;**18**:594–609.
23. Mills CD, Kincaid K, Alt JM, Heilman MJ, Hill AM. M-1/M-2 macrophages and the Th1/Th2 paradigm. *J Immunol* 2000;**164**:6166–73.
24. Palmieri EM, Gonzalez-Cotto M, Baseler WA, Davies LC, Ghesquiere B, Maio CM, Rice CM, Rouault TA, Cassel T, Higashi RM, et al. Nitric oxide orchestrates metabolic rewiring in M1 macrophages by targeting aconitase 2 and pyruvate dehydrogenase. *Nat Commun* 2020;**11**:698.
25. Padgett LE, Burg AR, Lei W, Tse HM. Loss of NADPH oxidase-derived superoxide skews macrophage phenotypes to delay type 1 diabetes. *Diabetes* 2015;**64**:937–46.
26. Feng Q, Xu M, Yu YY, Hou Y, Mi X, Sun YX, Ma S, Zuo XY, Shao LL, Hou M, et al. High-dose dexamethasone or all-trans-retinoic acid restores the balance of macrophages towards M2 in immune thrombocytopenia. *J Thromb Haemost* 2017;**15**:1845–58.
27. Zhang Y, Choksi S, Chen K, Pobezinskaya Y, Linnoila I, Liu ZG. ROS play a critical role in the differentiation of alternatively activated macrophages and the occurrence of tumor-associated macrophages. *Cell Res* 2013;**23**:898–914.
28. Park S, Jiang Z, Mortenson ED, Deng L, Radkevich-Brown O, Yang X, Sattar Y, Wang Y, Brown NK, Greene M, et al. The therapeutic effect of anti-HER2/neu antibody depends on both innate and adaptive immunity. *Cancer Cell* 2010;**18**:160–70.
29. Lawson MA, McDonald MM, Kovacic N, Hua Khoo W, Terry RL, Down J, Kaplan W, Paton-Hough J, Fellows C, Pettitt JA, et al. Osteoclasts control reactivation of dormant myeloma cells by remodelling the endosteal niche. *Nat Commun* 2015;**6**:8983.
30. Wang LC, Lo A, Scholler J, Sun J, Majumdar RS, Kapoor V, Antzis M, Cotner LA, Johnson LA, Durham AC, et al. Targeting fibroblast activation protein in tumor stroma with chimeric antigen receptor T cells can inhibit tumor growth and augment host immunity without severe toxicity. *Cancer Immunol Res* 2014;**2**:154–66.
31. Xie YJ, Dougan M, Jailkhani N, Ingram J, Fang T, Kummer L, Momin N, Pishesha N, Rickelt S, Hynes RO, et al. Nanobody-based CAR T cells that target the tumor microenvironment inhibit the growth of solid tumors in immunocompetent mice. *PNAS* 2019;**116**:7624–31.
32. Costa A, Kieffer Y, Scholer-Dahirel A, Pelon F, Bourachot B, Cardon M, Sirven P, Magagna I, Fuhrmann L, Bernard C, et al. Fibroblast heterogeneity and immunosuppressive environment in human breast cancer. *Cancer Cell* 2018;**33**, 463–479 e410.
33. von Herrath MG, Harrison LC. Antigen-induced regulatory T cells in autoimmunity. *Nat Rev Immunol* 2003;**3**:223–32.
34. Sakaguchi S, Sakaguchi N, Shimizu J, Yamazaki S, Sakihama T, Itoh M, Kuniyasu Y, Nomura T, Toda M, Takahashi T. Immunologic tolerance maintained by CD25+ CD4+ regulatory T cells: their common role in controlling autoimmunity, tumor immunity, and transplantation tolerance. *Immunol Rev* 2001;**182**:18–32.
35. Shevach EM. CD4+ CD25+ suppressor T cells: more questions than answers. *Nat Rev Immunol* 2002;**2**:389–400.
36. Zou W. Regulatory T cells, tumour immunity and immunotherapy. *Nat Rev Immunol* 2006;**6**:295–307.
37. Zou W. Immunosuppressive networks in the tumour environment and their therapeutic relevance. *Nat Rev Cancer* 2005;**5**:263–74.
38. Chao MP, Alizadeh AA, Tang C, Myklebust JH, Varghese B, Gill S, Jan M, Cha AC, Chan CK, Tan BT, et al. Anti-CD47 antibody synergizes with rituximab to promote phagocytosis and eradicate non-Hodgkin lymphoma. *Cell* 2010;**142**:699–713.
39. Guilliams M, Bruhns P, Saeys Y, Hammad H, Lambrecht BN. The function of Fcgamma receptors in dendritic cells and macrophages. *Nat Rev Immunol* 2014;**14**:94–108.
40. Mercogliano MF, De Martino M, Venturutti L, Rivas MA, Proietti CJ, Inurrigarro G, Frahm I, Allemand DH, Deza EG, Ares S, et al. TNFalpha-induced mucin 4 expression elicits trastuzumab resistance in HER2-positive breast cancer. *Clin Cancer Res* 2017;**23**:636–48.
41. Chew HY, De Lima PO, Gonzalez Cruz JL, Banushi B, Echejoh G, Hu L, Joseph SR, Lum B, Rae J, O'Donnell JS, et al. Endocytosis inhibition in humans to improve responses to ADCC-mediating antibodies. *Cell* 2020;**180**, 895–914 e827.
42. Collins DM, O'Donovan N, McGowan PM, O'Sullivan F, Duffy MJ, Crown J. Trastuzumab induces antibody-dependent cell-mediated cytotoxicity

(ADCC) in HER-2-non-amplified breast cancer cell lines. *Ann Oncol* 2012;**23**:1788–95.
43. Su S, Zhao J, Xing Y, Zhang X, Liu J, Ouyang Q, Chen J, Su F, Liu Q, Song E. Immune checkpoint inhibition overcomes ADCP-induced immunosuppression by macrophages. *Cell* 2018;**175**, 442–457 e423.
44. Lech M, Anders HJ. Macrophages and fibrosis: How resident and infiltrating mononuclear phagocytes orchestrate all phases of tissue injury and repair. *BBA* 2013;**1832**:989–97.
45. Mazzoni A, Bronte V, Visintin A, Spitzer JH, Apolloni E, Serafini P, Zanovello DM, Segal DM. Myeloid suppressor lines inhibit T cell responses by an NO-dependent mechanism. *J Immunol* 2002;**168**:689–95.
46. Bronte V, Zanovello P. Regulation of immune responses by L-arginine metabolism. *Nat Rev Immunol* 2005;**5**:641–54.
47. Bronte V, Serafini P, De Santo C, Marigo I, Tosello V, Mazzoni A, Segal DM, Staib C, Lowel M, Sutter G, et al. IL-4-induced arginase 1 suppresses alloreactive T cells in tumor-bearing mice. *J Immunol* 2003;**170**:270–8.
48. Kusmartsev S, Nefedova Y, Yoder D, Gabrilovich DI. Antigen-specific inhibition of CD8+ T cell response by immature myeloid cells in cancer is mediated by reactive oxygen species. *J Immunol* 2004;**172**:989–99.
49. Rodriguez PC, Zea AH, DeSalvo J, Culotta KS, Zabaleta J, Quiceno DG, Ochoa JB, Ochoa AC. L-arginine consumption by macrophages modulates the expression of CD3 zeta chain in T lymphocytes. *J Immunol* 2003;**171**:1232–9
50. Curiel TJ, Coukos G, Zou L, Alvarez X, Cheng P, Mottram P, Evdemon-Hogan M, Conejo-Garcia JR, Zhang L, Burow M, et al. Specific recruitment of regulatory T cells in ovarian carcinoma fosters immune privilege and predicts reduced survival. *Nat Med* 2004;**10**:942–9.
51. Kryczek I, Wei S, Zou L, Zhu G, Mottram P, Xu H, Chen L, Zou W. Cutting edge: induction of B7–H4 on APCs through IL-10: novel suppressive mode for regulatory T cells. *J Immunol* 2006;**177**:40–4.
52. Zou W, Machelon V, Coulomb-L'Hermin A, Borvak J, Nome F, Isaeva T, Wei S, Krzysiek R, Durand-Gasselin I, Gordon A, et al. Stromal-derived factor-1 in human tumors recruits and alters the function of plasmacytoid precursor dendritic cells. *Nat Med* 2001;**7**:1339–46.
53. Curiel TJ, Wei S, Dong H, Alvarez X, Cheng P, Mottram P, Krzysiek R, Knutson KL, Daniel B, Zimmermann MC, et al. Blockade of B7–H1 improves myeloid dendritic cell-mediated antitumor immunity. *Nat Med* 2003;**9**:562–7
54. Chen L. Co-inhibitory molecules of the B7-CD28 family in the control of T-cell immunity. *Nat Rev Immunol* 2004;**4**:336–47.
55. von Minckwitz G, Huang CS, Mano MS, Loibl S, Mamounas EP, Untch M, Wolmark N, Rastogi P, Schneeweiss A, Redondo A, et al. Trastuzumab emtansine for residual invasive HER2-positive breast cancer. *N Engl J Med* 2019;**380**:617–28.
56. Piccart-Gebhart MJ, Procter M, Leyland-Jones B, Goldhirsch A, Untch M, Smith I, Gianni L, Baselga J, Bell R, Jackisch C, et al. Trastuzumab after adjuvant chemotherapy in HER2-positive breast cancer. *N Engl J Med* 2005;**353**:1659–72.